Stoichiometry of the Vinblastine-Induced Self-Association of Calf Brain Tubulin†

George C. Na and Serge N. Timasheff*

ABSTRACT: The self-association of calf brain tubulin in PG buffer (10^{-2} M NaP_i and 10^{-4} M GTP, pH 7.0) induced by the antimitotic drug vinblastine has been investigated by velocity sedimentation. Schlieren sedimentation patterns were examined at low vinblastine concentrations where the boundary resolves into a bimodal one and at high vinblastine concentration where a single forward-skewed peak prevails. Weight-average sedimentation coefficients of tubulin were determined as a function of protein concentration, the results fitting well a self-association model of an indefinite isodesmic mechanism. This was confirmed by computer simulation of the sedimentation boundary profiles.

Vinblastine is an alkaloid isolated from the plant *Vinca rosea* Linn and found to be effective in the treatment of some neoplastic diseases (Johnson et al., 1960; Cutts et al., 1960; Warwick et al., 1960). In vivo and in vitro studies have shown that the administration of vinblastine can disrupt cell spindles and arrest cells at the metaphase (Palmer et al., 1960; Cutts, 1961). Furthermore, addition of vinblastine induces the formation in cells of a highly ordered paracrystalline structure composed of vinblastine and tubulin, the protein component of microtubules (Bensch & Malawista, 1968, 1969; Malawista & Sato, 1969; Bryan, 1971, 1972a,b; Behnke & Forer, 1972; Nagayama & Dales, 1970; Krishan & Hsu, 1971; Dales et al., 1973). These findings have suggested that the antineoplastic action of vinblastine stems from its interaction with the cell microtubule protein and the resulting disruption of the mitotic spindles.

Following the initial purification of tubulin (Weisenberg et al., 1968), Weisenberg & Timasheff (1970) demonstrated that, in PG buffer,[1] each tubulin dimer[2] can bind no more than two vinblastine molecules, the protein being able to undergo then a stepwise self-association. It was later shown by Lee et al. (1975), Wilson et al. (1975), and Bhattacharyya & Wolff (1976) that each tubulin dimer has two strong vinblastine binding sites. Besides being able to bind to tubulin, vinblastine has also been shown to inhibit microtubule assembly in vitro (Owellen et al., 1976; Himes et al., 1976; Bhattacharyya & Wolff, 1976). Under certain buffer conditions, vinblastine can also induce tubulin to self-assemble in vitro into coiled and tubular structures, analogous to the paracrystalline assemblies observed in vivo (Bensch et al., 1969; Marantz & Shelanski, 1970; Warfield & Bouck, 1974).

While the evidence on the general mechanism of the antimitotic activity of vinblastine seems to be overwhelming, little is known about the interaction mechanism at the molecular level. It is not clear, for example, how tubulin assembles into the paracrystalline aggregates; nor is the manner known in which binding of the vinblastine molecule is energetically coupled to the disruption of microtubules and to the induced self-association of tubulin. While both magnesium ions and GTP are essential for microtubule assembly, their role in the vinblastine-induced tubulin self-association is unclear. In seeking answers to these questions, we have initiated a detailed physicochemical study of vinblastine–tubulin interactions and of the vinblastine-induced tubulin self-association. Confronted with this complex association system, which very probably is multidimensional and may involve the participation of several ligands, our approach has been that of focusing on one isolated homologous interaction at a time, with the hope that a detailed characterization of the individual interactions will make it possible to link them and to present an integrated view of the system. In this paper, we are reporting on the velocity sedimentation examination of the stoichiometry and pathway of the vinblastine-induced self-association of tubulin. A preliminary report of these studies has been presented earlier (Na & Timasheff, 1978). The following paper (Na & Timasheff, 1980) is devoted to an analysis of the association thermodynamics and of the energy linkages between vinblastine binding and the self-association reactions.

Materials and Methods

Calf brains were obtained from freshly slaughtered animals, kept on ice, and used within 1 h from sacrifice. Sigma II-S grade guanosine 5′-triphosphate (GTP), 95–97% pure, was used. Special ultrapure grade ammonium sulfate and sucrose were obtained from Schwarz/Mann. Ultrapure guanidine hydrochloride was purchased from Heico Co., and its solution was filtered through a sintered glass funnel before use. Vinblastine sulfate was a gift from Eli-Lilly and Co., through the courtesy of Dr. K. Gerson, and was used without further purification. All other chemicals used were of reagent grade.

Preparation of Calf Brain Tubulin. Calf brain tubulin was prepared by the method originally developed by Weisenberg et al. (1968) and Weisenberg & Timasheff (1970) as modified by Lee et al. (1973). The procedure was further modified by using 0.5 mM instead of 5 mM $MgCl_2$ throughout the preparation. The tubulin obtained was stored in 1 M sucrose–PMG buffer (10^{-2} M NaP_i, 5×10^{-4} M $MgCl_2$, and 10^{-4} M GTP, pH 7.0) (Frigon & Lee, 1972) under liquid nitrogen until use. Before each experiment, the tubulin solution was made free of sucrose and brought to equilibrium with the experimental buffer. For the experiments at hand, it was essential that tubulin be fully equilibrated with a known concentration of free vinblastine (Wyman, 1964; Lee & Timasheff, 1977). This was accomplished by equilibrating the protein, usually 20 mg, with a batch of Sephadex G-25 gel, which had been equili-

† From the Graduate Department of Biochemistry, Brandeis University, Waltham, Massachusetts 02254. *Received July 11, 1979.* Supported by National Institutes of Health grants (CA 16707 and GM 14603) and a National Health Service Award (CA 05538). This paper is Publication No. 1296.

[1] Abbreviations used: PG, 0.01 M NaP_i and 10^{-4} M GTP, pH 7.0; Gdn·HCl, guanidine hydrochloride; $NaDodSO_4$, sodium dodecyl sulfate.

[2] In this context, dimer refers to the 110 000 molecular weight stable kinetic unit normally isolated when pure native tubulin is prepared.

0006-2960/80/0419-1347$01.00/0

brated with the desired concentration of vinblastine, followed by elution through a 0.9 × 20 cm Sephadex G-25 gel column. Aliquots of 0.5 mL were collected from the column. The equilibration was periodically checked with the photoelectric scanner of the analytical ultracentrifuge. In the solutions used, only vinblastine absorbs at 320 nm. Therefore, for a protein sample well equilibrated with a high concentration of vinblastine, the absorptivity at 320 nm of the solvent centripetal to the protein boundary should be essentially equal to that of the equilibrating buffer.

The protein concentration was determined by two different methods. A small aliquot of the protein was diluted in 6 M Gdn·HCl, followed by measurement of the solution absorbance at 275 nm with a Cary 118 spectrophotometer. The protein concentration was then calculated by using an extinction coefficient of 1.03 mL mg^{-1} cm^{-1} (G. C. Na and S. N. Timasheff, unpublished experiments). For tubulin equilibrated with vinblastine, the contribution to the absorption at 275 nm from the vinblastine molecules bound to the protein was calculated to be very small when the concentration of free vinblastine in the solution was less than 1×10^{-4} M. This was confirmed by the single linear relationship found between the interference fringe shift or the Schlieren peak area in the ultracentrifuge and the protein concentration determined from the solution absorbance at 275 nm. When the concentration of free vinblastine in the solution was increased to 1×10^{-4} M or higher, the absorbance contribution from the bound vinblastine became significant. In such experiments the protein concentration was determined by the interference fringe shift of the Schlieren peak area in the ultracentrifuge, since these are not affected by the presence of vinblastine.

Velocity Sedimentation. Velocity sedimentation experiments were performed in a Beckman Model E analytical ultracentrifuge equipped with electronic speed control and RTIC temperature control. A Kel-F centerpiece and quartz windows were used with Schlieren optics at protein concentrations above 4 mg/mL, whereas sapphire windows were used with Raleigh optics at protein concentrations below 4 mg/mL. Sedimentation boundary images were recorded on Kodak metallographic or type II-G spectroscopic plates. The second moment of the sedimentation boundary was established by numerical integration of the data measured from the photographic plate with a Nikon Model 6C microcomparator equipped with an Elk Model 9200 precision digital positioner and an electronic digital display.

It should be emphasized that for a rapidly equilibrating ligand-induced self-association system, there should exist practically no concentration gradient of either the macromolecule or the solution ligand in the plateau region. Consequently, despite the formation of a concentration gradient of free ligand across the sedimentation boundary and the resolution of the sedimentation pattern into a bimodal one, the displacement of the second moment corresponds rigorously to the weight-average sedimentation at the total macromolecule and ligand concentrations found in the plateau region (Goldberg, 1953).

Results

Effect of Vinblastine on the Sedimentation Behavior of Tubulin. The physicochemical and biochemical properties of the calf brain tubulin isolated by the modified Weisenberg procedure have been well characterized (Lee et al., 1973; Frigon & Timasheff, 1975a; Lee & Timasheff, 1975). In $NaDodSO_4$–polyacrylamide gel electrophoresis this protein is more than 99% homogeneous. In PG buffer, it exists as a stable dimer of 110 000 molecular weight and sediments as a single rather symmetrical peak with $s^0_{20,w} = 5.8$ S (Figure 1a). The concentration dependence of the sedimentation coefficient below 10 mg/mL is depicted in Figure 2. It obeys the standard equation (Schachman, 1959)

$$s = s^0(1 - gc) \quad (1)$$

with a value of the hydrodynamic nonideality constant, g, of 0.018 mL/mg (Frigon & Timasheff, 1975a).

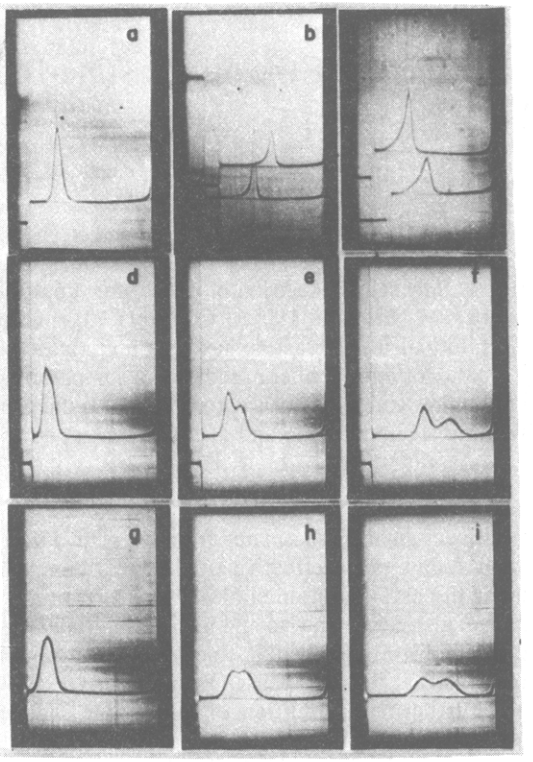

FIGURE 1: Velocity sedimentation patterns of tubulin. (a) Tubulin (12 mg/mL) was equilibrated with PG (pH 7.0) buffer and then sedimented at 60 000 rpm; the picture was taken at a bar angle of 70°, 40 min after reaching speed. (b) Tubulin was equilibrated with PG–2×10^{-4} M vinblastine (pH 7.0) buffer and then sedimented at 60 000 rpm; the picture was taken at a bar angle of 70°, 24 min after reaching speed. The protein concentration was 6.7 mg/mL for the top pattern and 8.3 mg/mL for the bottom one. (c) Tubulin was equilibrated with PG–2.5×10^{-5} M vinblastine (pH 7.0) and then sedimented at 60 000 rpm; the picture was taken 16 min after reaching speed. The protein concentration was 8.5 mg/mL for the top pattern and 6.8 mg/mL for the bottom one. (d–f) Tubulin (10.3 mg/mL) was equilibrated with PG–1×10^{-5} M vinblastine (pH 7.0) buffer and then sedimented at 60 000 rpm. Pictures were taken at a bar angle of 65°, 16, 32, and 64 min after reaching top speed. (g–i) Same as (d–f), except that the centrifugation was at 48 000 rpm and the pictures were taken at 32, 64, and 104 min after reaching speed.

Parts b and c of Figure 1 represent typical sedimentation profiles obtained with tubulin that had been equilibrated with 2×10^{-4} and 2.5×10^{-5} M free vinblastine in PG buffer. The protein exhibits a single, forward-skewed peak with a sharp leading edge and a sloped trailing edge extending toward the meniscus. This characteristic boundary shape persists throughout the entire range of protein concentration studied, i.e., from 0.8 to 12 mg/mL as well as up to the highest vinblastine concentration used, namely, 5×10^{-4} M.

A decrease in the free vinblastine concentration to 1×10^{-5} M or below leads to a gradual transition of the sedimentation boundary into a bimodal one. The actual concentration of unbound vinblastine where the bimodality becomes prominent is a function of both the total protein concentration and the velocity of the centrifugation. At a fixed concentration of free vinblastine, resolution was favored by higher protein concentrations and higher rotor speeds, as depicted in parts d–i of

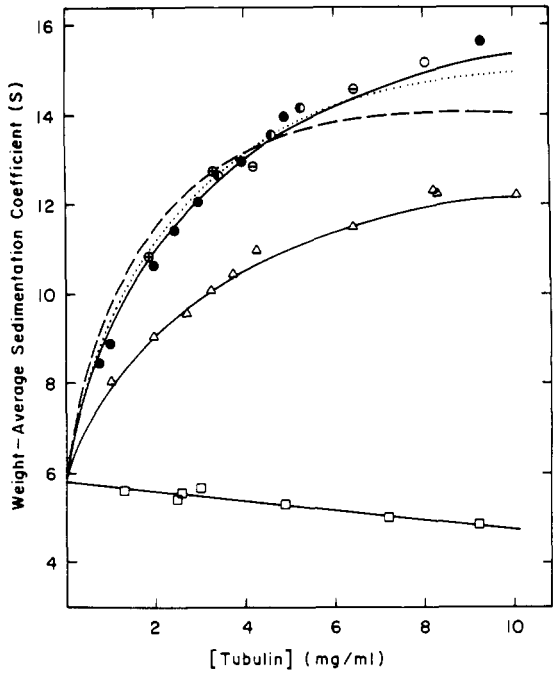

FIGURE 2: Total protein concentration dependence of the weight-average sedimentation coefficient ($\bar{s}_{20,w}$) of tubulin in the presence of vinblastine. Tubulin was equilibrated with PG–1 × 10^{-4} M vinblastine (○) or PG–5 × 10^{-5} M vinblastine (△) prior to sedimentation. Weight-average sedimentation coefficients were determined by integrating the Schlieren or Raleigh sedimentation patterns as described under Materials and Methods. The data with 1 × 10^{-4} M vinblastine were obtained at different rotor speeds; these were (●) 60 000, (⊕) 56 000, (◐) 52 000, (⊖) 48 000, and (○) 40 000 rpm. The solid curves represent the calculated least-squares fitting of the $s_{20,w}$ by the isodesmic, indefinite self-association mechanism as described in the text, where K_2^{app} = 1.0 × 10^5 and 5.2 × 10^4 M^{-1} for 10^{-4} and 5 × 10^{-5} M vinblastine, respectively. The dashed and dotted lines are least-squares fittings of data at 1 × 10^{-4} M vinblastine by a limited isodesmic self-association which terminates at n = 10 and 15, respectively. The protein concentration dependence of the sedimentation coefficient of tubulin equilibrated with PG (pH 7.0) buffer [taken from Frigon & Timasheff (1975a)] is also shown (□), where the straight line represents the linear least-squares fitting of the data.

Figure 1. Within a single centrifugation experiment, resolution also increased with increasing centrifugation time. As shown in parts d–f of Figure 1 at a free vinblastine concentration of 1 × 10^{-5} M, the sedimentation boundary is unimodal at the beginning of centrifugation; bimodality first appears after ~20 min of centrifugation at 60 000 rpm. The time interval required for bimodality to appear is also a function of the speed of centrifugation. This is evident in parts g–i of Figure 1, in which all the conditions are identical with those of parts d–f of Figure 1, except that the rotor speed has been lowered to 48 000 rpm. At this speed, peak resolution becomes evident only ~56 min after reaching full speed. The sedimentation coefficients, $s_{20,w}$, of the apexes of the two peaks in both parts d–f and parts g–i of Figure 1 were measured as 5.1 and 7.7 S, which, after correction for the concentration dependence according to eq 1, correspond quite well to those of the tubulin 110 000 molecular weight dimer and the 220 000 molecular weight tetramer, the two species found to predominate under the conditions of these experiments. The area distribution between the fast and slow peaks under the two bimodal sedimentation reaction boundaries was determined with a Du Pont curve resolver. For the sedimentation boundary shown in Figure 1f, the slow and fast moving peaks contained 45 and 55% of the total area under the boundary, respectively. The corresponding values for the boundary in Figure 1i were found to be 35 and 65%.

Model of the Self-Association. The single, forward-skewed peak seen at high vinblastine concentrations is similar in shape to the simulated sedimentation patterns calculated by Holloway & Cox (1974) for a model of indefinite self-association of the type

$$\begin{aligned} A + A &\rightleftharpoons A_2 & K_2 &= \frac{[A_2]}{[A]^2} \\ A_2 + A &\rightleftharpoons A_3 & K_3 &= \frac{[A_3]}{[A_2][A]} \\ \vdots \quad & \quad \vdots & \vdots & \\ A_{n-1} + A &\rightleftharpoons A_n & K_n &= \frac{[A_n]}{[A_{n-1}][A]} \end{aligned} \qquad (2)$$

where A_i and $[A_i]$ denote the ith aggregate and its molar concentration. K_i's are the association constants for the formation of succesive bonds between monomer and $(i-1)$-mer. If all the K_i's are equal, the self-association is referred to as isodesmic (Chun et al., 1969; Chun & Kim, 1969; Reisler et al., 1970).

The analysis of such associations lends itself more conveniently to the use of mass concentration units. Expressing the concentration of the ith aggregate, C_i, in units of milligrams per milliliter, the formation constant of the ith aggregate, k_i, for an isodesmic system becomes

$$k_i = C_i/C_1^i = i(k_2/2)^{i-1} \qquad (3)$$

$$k_2 = C_2/C_1^2 = 2K_2/M_1 \qquad (4)$$

where M_1 is the molecular weight of the monomeric unit in the self-association reaction. In the case of tubulin, M_1 is taken as 110 000 since it is the stable kinetic unit in the polymerization reaction;[3] K_2 retains its previous definition. For an isodesmic self-association, the total weight concentration of the protein, C_0, can be expressed as

$$C_0 = \sum_{i=1}^{n} C_i = \sum_{i=1}^{n} i(k_2/2)^{i-1} C_1^i \qquad (5)$$

If the self-association is indefinite, the infinite series must converge, i.e., $k_2C_1/2 < 1$, and it reduces to (Reisler et al., 1970)

$$C_0 = C_1/[1 - (k_2C_1/2)]^2 \qquad (6)$$

In this way, it is possible to calculate directly from the binomial equation the concentration of monomer and each ith polymer, given the total protein concentration C_0 and the dimer formation constant k_2. For a limited isodesmic self-association which terminates at a given polymer stoichiometry, the concentration of each species can be obtained by solving eq 5 numerically through a binary search method.

In analytical methods which depend on molecular transport, such as velocity ultracentrifugation, the mass distribution of species in a reversibly self-associating system can be related to the weight-average sedimentation coefficient by

$$\bar{s} = \sum_{i=1}^{n} s_i C_i / \sum_{i=1}^{n} C_i \qquad (7)$$

where s_i is the sedimentation coefficient of the ith associated species. Combination of eq 1, 3, 5, and 7 leads to

[3] For tubulin, the kinetically stable unit in solution is the 110 000 molecular weight dimer. Under the conditions of our experiments it remains stable, since the free energy of intersubunit interaction in the dimer is –7.8 kcal/mol at 4.6 °C (Detrich & Williams, 1978). No detectable dissociation of the subunits should occur, therefore, above 0.8 mg/mL tubulin, which is the lowest protein concentration used in this study.

$$\bar{s} = \sum_{i=1}^{n} s_i^0(1 - g_i C_0) i(k_2/2)^{i-1} C_1^{\,i} / \sum_{i=1}^{n} i(k_2/2)^{i-1} C_1^{\,i} \quad (8)$$

where g_i is the hydrodynamic nonideality constant of the ith species.

For an indefinite self-association, $\bar{s}$ is calculated by continuously counting new terms corresponding to species of higher degrees of association in eq 8 until practically all of the protein (e.g., 99.9%) is accounted for (Holloway & Cox, 1974). For a stepwise self-association with a limited number of species, C_i and thus $\bar{s}$ can be obtained with a simple binary search method (Cox, 1978). In carrying out this calculation with eq 8, the experimentally obtained values of $s_1^0 = 5.8$ S and $g_1 = 0.018$ mL/mg can be used directly. However, there are no readily available experimental values of s_i^0 and g_i for the associated species. In the analysis that follows, it was assumed that the sedimentation coefficient of the ith aggregate, s_i^0, is a simple function of $s_1^0 = 5.8$ S, namely

$$s_i^0 = i^{2/3} s_1^0 \quad (9)$$

and that the hydrodynamic nonideality constants, g_i, for all polymeric species are identical with that of the monomer. Equation 9 is derived from the Svedberg equation with the assumption that all polymeric species have the same partial specific volume as the monomer, as well as spherical symmetry. This is obviously not rigorously correct. Introduction of further parameters into the analysis at this stage, however, would only complicate the calculation without producing any new insight into the mechanism of the self-association. The simplest model described above was therefore used in the analysis that follows.

Fitting of Sedimentation Data to the Model. The protein concentration dependence of the weight-average sedimentation coefficients of tubulin was determined in the presence of various constant concentrations of free vinblastine. Typical results obtained on tubulin that had been equilibrated with 1×10^{-4} and 5×10^{-5} M vinblastine in PG buffer are shown in Figure 2. At this level of free vinblastine, tubulin exhibits a single forward-skewed peak up to the highest protein concentration studied, i.e., 12 mg/mL. As shown in Figure 2, the weight-average sedimentation coefficient increases hyperbolically with increasing protein concentration. These data were analyzed in terms of the isodesmic, indefinite self-association reaction mechanism described in the previous section. The solid lines of Figure 2 represent the least-squares fitting of the experimental data. It is evident that this model can accommodate the data very well. The apparent dimer formation constant, k_2, derived from this calculation was found to be 0.95 mL/mg or 5.2×10^4 M^{-1} in the presence of 5×10^{-5} M vinblastine and 1.1×10^5 M^{-1} in the presence of 1×10^{-4} M vinblastine. This corresponds to standard free energy changes of $\Delta G° = -6.3$ and -6.8 kcal/mol, respectively.

The sedimentation velocity data obtained at 1×10^{-4} M vinblastine were also analyzed in terms of a model in which an isodesmic self-association terminates at a given stoichiometry without any favorable free energy change for the formation of the end product. The least-squares fittings by the stoichiometries of 10 and 15 are depicted in Figure 2 by the dashed and dotted lines, respectively. Because of the absence of higher polymer species, for a limited isodesmic self-association, the weight-average sedimentation coefficient reaches a plateau at a lower total protein concentration. Consequently, one has to increase k_2 to obtain a better fit to the experimental data at high protein concentrations. This, however, brings on a simultaneous deterioration of the fitting at lower protein concentrations. Table I summarizes the fitted apparent association constants and degrees of deviation for the above two

Table I: Least-Squares Fitting of Weight-Average Sedimentation Velocity Data[a]

stoichiometry	k_2 (mL/mg)	SSD[b]
10	2.31	6.81
12	2.16	3.69
15	2.03	1.82
18	2.01	1.22
20	1.98	1.02
∞	1.97	0.84

[a] Isodesmic association was assumed for all stoichiometries. [b] Sum of squares of deviation.

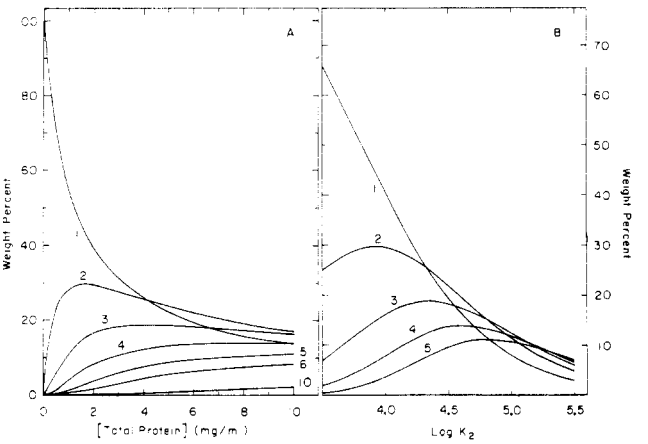

FIGURE 3: Mass distribution of tubulin among different size polymers for an isodesmic, indefinite self-association. (A) Dependence on the total protein concentration; $K_2^{app} = 5.2 \times 10^4$ M^{-1}. (B) Dependence on the polymerization constants; total protein concentration = 10 mg/mL. The number next to each curve is the corresponding degree of polymerization.

curves as well as several other association stoichiometries. Apparently the deviation between experimental data and least-squares fitted curves gradually diminishes with increasing association stoichiometries up to 20. Beyond this, the calculated curves are practically nondifferentiable from that of the indefinite self-association.

Figure 3A depicts the mass distribution of tubulin present in the different size polymeric species as a function of the total protein concentration, calculated in terms of the isodesmic indefinite self-association mechanism described above. With $k_2 = 0.95$ mL/mg, it is found that the 110000 molecular weight tubulin dimer is the predominant species at low protein concentrations. Its weight percentage decreases continuously with increasing protein concentration. In the case of tubulin tetramers, M_r 220000, the weight percentage increases from 0 to 30% at 1.5 mg/mL, where it reaches a maximum before slowly decreasing. Below 10 mg/mL total protein concentration, the sum of the aggregates with a degree of polymerization greater than 10 (M_r 1.1×10^6) never exceeded 5% of the total protein by weight. With increasing protein concentration, the protein becomes more evenly distributed among different size polymers. A plot of the percentage distributions of dimers, tetramers, hexamers, octamers, and decamers as a function of k_2 at a total protein concentration of 10 mg/mL is shown in Figure 3B. It is evident that the protein exists predominantly as smaller species at lower association constants. It becomes more evenly distributed among different size polymers as the association constant is increased.

Simulation of Velocity Sedimentation Profiles. Ever since Gilbert's (1955, 1959) first description of the calculation of Schlieren sedimentation profiles using an asymptotic approach, the technique of numerical simulation of velocity sedimentation

patterns has been used extensively and fruitfully in the deduction of mechanisms of biomacromolecule associations. Indeed, the sedimentation boundaries of systems undergoing different modes of association often possess strikingly different characteristics. As a result, a precise comparison of the experimental sedimentation pattern with those calculated with a high-speed digital computer can provide valuable information about the general reaction mechanism of the association.

Since the sedimentation patterns of tubulin in the presence of high concentrations of vinblastine are quite similar to those calculated by Holloway & Cox (1974) for an isodesmic self-associating system, sedimentation boundaries were generated for the tubulin–vinblastine self-association system according to that model through numerical simulation, using the reaction parameters obtained above from the analysis of the weight-average sedimentation coefficients. In calculating the centrifugation boundary of a rapidly self-associating system, the transport process can be treated similarly to that of a homogeneous system. The only adjustment to be made is that local transport be described in terms of the weight-average sedimentation coefficient and the average diffusion coefficient defined by (Cox, 1978)

$$\bar{D} = \sum_{i=1}^{n} iD_iC_i / \sum_{i=1}^{n} iC_i \qquad (10)$$

where D_i is the diffusion coefficient of the ith aggregate. For tubulin dimer, the diffusion coefficient can be estimated from the Svedberg equation by using a partial specific volume of $\bar{v} = 0.736$ mL/g (Lee & Timasheff, 1974). The value of D_1, estimated by this method, is 4.87×10^{-7} cm^2/s, in good agreement with the value of 4.41×10^{-7} cm^2/s reported by Gethner et al. (1977) from laser light scattering experiments. The diffusion coefficients of the associated species can be estimated from the relation

$$D_i = i^{-1/3}D_1 \qquad (11)$$

again assuming spherical symmetry for all species. For a ligand-mediated self-association, the weight-average sedimentation coefficient is a function of both the total protein concentration and that of the free ligand. It can either be calculated according to a given reaction mechanism as described above or be obtained experimentally as shown in Figure 2.

The simulation process was started by first tabulating $\bar{s}$ and $\bar{D}$ as a function of total protein concentration. The numerical process of Cox (1978) was then applied to an initial protein concentration profile in a hypothetical sector-shaped centrifuge cell which was divided into compartments of equal length. The results of the calculations for the case of an initial hypersharp boundary formed by a 10 mg/mL tubulin solution are shown in Figure 4A. The simulated velocity patterns were calculated for 510, 964, and 1475 s after formation of the synthetic boundary. It is evident that the resulting boundary profiles, with a steep leading edge and a sloped trailing edge, possess striking similarities to those shown in parts b and c of Figure 1.

Although the results obtained with an initial hypersharp boundary can be compared directly with those of a synthetic boundary run, centrifugation experiments as normally performed are subject to an inhomogeneous centrifugal force during acceleration and are also limited in their diffusion at the meniscus. Gilbert & Gilbert (1973) have proposed that these difficulties can be circumvented by using as a starting point for the simulation process an initial experimentally measured boundary profile which is devoid of protein near the meniscus. The results of such calculations for the tubulin–vinblastine system are shown in Figure 4B. In this simulation, the initial boundary fed into the computer was that of tubulin which had been equilibrated with 5×10^{-5} M vinblastine in PG buffer and centrifuged at 52000 rpm for 32 min. The simulation process was then allowed to proceed for a predetermined period of time. The numerically calculated boundary profile for 8 min following the initial boundary is shown by the solid line in Figure 4B. The reasonably good agreement with the experimental pattern further supports the validity of the isodesmic self-association mechanism for this reaction.

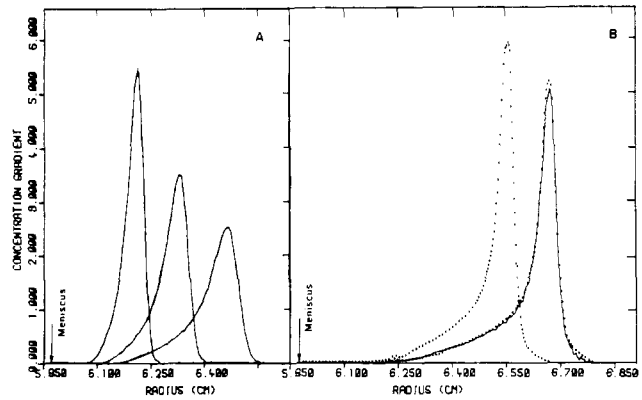

FIGURE 4: Computer simulation of the velocity sedimentation profiles of tubulin in a sector-shaped cell. The ordinates for both parts A and B are in random units, whereas the abcissa represents the radial distance from the center of rotation. (A) The simulation process was started with an initial sharp boundary of 10 mg/mL set at 6.09 cm from the center of rotation. It was then subjected to simulated sedimentation at 52000 rpm according to the isodesmic indefinite self-association model as described by the curve of $K_2 = 5.2 \times 10^4$ M^{-1} shown in Figure 2. The resulting Schlieren sedimentation patterns were calculated for 510, 964, and 1475 s of centrifugation, respectively. (B) The simulation process was started after 32 min of sedimentation. The dotted line patterns are experimental Schlieren patterns after 32 and 40 min of sedimentation after reaching speed of tubulin (12 mg/mL) equilibrated with PG–5×10^{-5} M vinblastine. The early sedimentation pattern was used as the initial boundary for computer simulation according to the isodesmic, indefinite self-association model, using the $s_{20,w}$ values depicted by the curve in Figure 2. The simulated sedimentation was allowed to proceed for 8 min. The resulting simulated sedimentation pattern (solid line) is to be compared with the second experimentally obtained sedimentation pattern.

It should be emphasized that the numerical simulation process was performed under the assumptions that the association reaction has a very short relaxation time and that it is independent of the hydrodynamic pressure generated in the centrifuge cell. These factors, together with the assumptions made in obtaining s_i and D_i for the various associated species, may contribute to the minor disagreements between the experimental and numerically simulated boundary profiles. The presence of these uncertainties makes it difficult to derive any further information on the molecular structure of the associated species through rigorous comparison between the experimental and simulated sedimentation patterns.

Discussion

The self-association of tubulin described in this paper is induced by strong interactions with vinblastine, since a free ligand concentration equimolar with the protein is sufficient to induce polymerization. The bimodal sedimentation patterns observed at low concentrations of free vinblastine possess the characteristics of those generated by a strong perturbation of unbound ligand concentration across the sedimentation boundary as described by Cann & Goad (1970a,b, 1972) and Cann & Kegeles (1974). The resolution of the sedimentation boundary into two peaks is favored by an increase in total

protein concentration, a decrease in free ligand concentration, and an increase in rotor speed, i.e., a decrease in the length of the experiment. At any given set of conditions, bimodality is favored by an increase in the sedimentation time and the accompanying broadening of the boundary. What gives rise to this behavior? A descriptive understanding of the phenomenon can be gathered from a simultaneous consideration of the sedimentation process and the reaction equilibrium. Cann & Goad (1972) have deduced that the bimodality arises from the active transport of the macromolecules and a depletion of unbound ligand from the trailing part of the boundary. We can conceive of the protein as a ligand carrier acting in the following way. Let a protein monomer bind ligand; this induces it to self-associate into polymers, which then sediment faster toward the bottom of the cell. Simultaneously, in maintaining the reaction equilibrium, polymers within the boundary, where total protein concentration is lower than in the plateau region, dissociate into monomers which then lag behind. According to the linkage theory, if a self-association is enhanced by ligand binding, the ligand must bind much more strongly to the polymers than to the monomers (Wyman, 1964; Lee & Timasheff, 1977). As a result, the active transport of the macromolecules, combined with the maintenance of the reaction equilibrium throughout the boundary, serves essentially as a ligand pump which constantly removes unbound ligand from the trailing region to the leading region of the reaction boundary. When there is no large excess of ligand present, this generates a concentration gradient of unbound ligand. At the beginning of the experiment, the boundary is sharp and the ligand gradient can be easily annihilated by back diffusion, with the result that no ligand gradient is formed. As the sedimentation boundary broadens, however, the diffusion process can no longer balance the gradient generated. By use of similar arguments, it becomes clear that lower total ligand concentrations, higher total protein concentrations, and faster rotor speeds can all contribute toward the formation of a stable concentration gradient of unbound ligand across the boundary.

The depletion of free ligand centripetal to the sedimentation boundary can also be understood through considering the protein species pelleted at the bottom of the cell. Let us consider a simple asymptotic sedimentation of a ligand-induced monomer–dimer self-associating system. At the beginning, monomers and dimers are in equilibrium with each other and with the free ligand. After application of a centrifugal field for an infinitesimally short interval, some of the macromolecules will be pelleted at the bottom of the cell. For a self-associating system, the mass ratio of dimer to monomer pelleted at the bottom of the cell is higher than the mass ratio of dimer to monomer in the solution. This is simply because the dimers sediment faster than the monomers. According to the Wyman linkage theory, for a unit weight of macromolecule more ligand is bound to the dimers than to the monomers. Consequently, the molar ratio of ligand bound to macromolecules that pellet at the bottom is higher than that found in the plateau solution. This extra amount of ligand pelleted must be taken from the region centripetal to the macromolecule boundary, since in the plateau area neither the macromolecule nor the ligand will change its concentration, other than as a result of radial dilution. Within the boundary, reequilibration of monomers to dimers will occur, with the binding of some free ligand. Since the dimer sediments faster than the monomer, a repetition of the process will result in ligand depletion in the boundary region.

An important corollary of the above analysis is that, for a ligand-induced self-associating system, the concentration of unbound ligand left in the supernatant after complete depletion of macromolecules by sedimentation will be lower than the concentration of unbound ligand originally present in the solution. Consequently, it is erroneous to use macromolecule depletion as a method to derive the ligand-binding constant in a ligand-induced self-associating system.

Why does a concentration gradient of unbound ligand across a reaction boundary result in a bimodal sedimentation pattern? A qualitative explanation can be gleaned from an examination of Figure 2. At a fixed concentration of unbound ligand, $\bar{s}_{20,w}$ increases hyperbolically with increasing protein concentration. At any given protein concentration, such curves obtained at various ligand concentrations are displaced toward higher $\bar{s}$ values with an increase in free ligand concentration [see also Figure 1 of the subsequent paper by Na & Timasheff (1980)]. This indicates, of course, stronger self-association. Consequently, if the unbound ligand concentration increases with increasing protein concentration across a sedimentation boundary, the resulting dependence of $s_{20,w}$ on protein concentration will no longer follow one of the curves of Figure 2, but it will shift across several curves, following the upper ones at higher protein concentration and the lower curves at low protein concentration. A consequence of this behavior is that the leading edge of the boundary will sediment considerably faster than the trailing edge. If the free ligand concentration gradient is sharp, e.g., if ligand is seriously depleted by strong interaction with the rapidly sedimenting aggregates, the result may be a sigmoidal dependence of $\bar{s}_{20,w}$ on protein concentration. Sigmoidal curves of $\bar{s}_{20,w}$ vs. protein concentration have been observed frequently (Townend et al., 1960; Frigon & Timasheff, 1975a) for Gilbert-type self-associations with positive cooperative interaction of macromolecules (Gilbert, 1955, 1959, 1963). Although the origins of the sigmoidal curves are different, due to an unbound ligand concentration gradient in one case and to cooperative interactions in the other case, they both must result in bimodal sedimentation patterns, since the Schlieren pattern is directly related to a plot of dc/ds as a function of s (Gilbert, 1955). Indeed, in computer simulations of sedimentation boundaries for all types of associations, the only parameters of the self-association reaction required are the dependences of $\bar{s}_{20,w}$ and $\bar{D}_{20,w}$ on protein concentration (Cox, 1978). Adoption of a simple relation between s and D, such as that of the Svedberg equation, leads to a direct correspondence between a plot of $\bar{s}_{20,w}$ vs. protein concentration and a sedimentation boundary of a specific shape. It should be pointed out that a major difference does exist between these two types of bimodal sedimentation boundaries, and it can be used as a diagnostic tool to differentiate between these two types of mechanisms. In the bimodal sedimentation patterns generated by cooperative self-association described by Gilbert (1955) and observed in the cases of β-lactoglobulin (Townend et al., 1960), the myosin fibril (Josephs & Harrington, 1968), and indeed the Mg^{2+}-induced self-association of tubulin to form the double-ring structure (Frigon & Timasheff, 1975a,b), the bimodality appears from the moment that the boundary emerges from the meniscus. On the other hand, when the bimodal pattern is generated by a free ligand concentration gradient as described by Cann & Goad (1970a) such as in the case of the vinblastine-induced tubulin polymerization, the boundary emerges from the meniscus as a single peak which gradually spreads and resolves into a bimodal one. The reason for this difference is that, for a cooperative self-association, the sigmoidal dependence of $\bar{s}$ on the protein concentration exists

from the beginning of the centrifugation, whereas in the latter case it is a consequence of the generation of a free ligand concentration gradient which can occur only after a finite time of centrifugation. These considerations give only a qualitative understanding of the reasons why, at low free vinblastine concentration, sedimentation patterns become bimodal. A quantitative examination and computer simulation of the bimodal sedimentation patterns, following the method of Cann & Goad (1970a), are presently in progress in our laboratory.

The second type of reaction boundary, characterized by a single, forward-skewed peak, observed at high concentrations of free vinblastine is essentially identical with that predicted by Holloway & Cox (1974) for a stepwise indefinite self-association. In our numerical simulation studies, both our experimental data of the protein concentration dependence of $\bar{s}_{20,w}$ and the sedimentation boundary profiles can be very well fitted in terms of this mechanism. The monotone hyperbolic increase of $\bar{s}_{20,w}$ with protein concentration indicates that, for the vinblastine-induced self-association, there is no energetically favorable end product such as the ring structure seen in the Mg^{2+}-induced tubulin self-association (Frigon & Timasheff, 1975a,b). However, the present data in themselves cannot exclude the possibility that the isodesmic self-association of tubulin terminates at some given polymer size greater than 20, with the concentration dependence of $\bar{s}_{20,w}$ and the sedimentation boundary profiles remaining essentially identical with those of an indefinite mechanism. While possible, such a mechanism is not plausible, since it would almost necessarily require a termination step that would not affect the overall thermodynamics of the chain growth reaction and would not favor thermodynamically the formation of the end product.

At this point, it seems worthwhile to reemphasize that, in the present study, magnesium ions were absent from the medium. The early studies of Weisenberg & Timasheff (1970) have indicated that the self-association of tubulin is strongly enhanced when both Mg^{2+} and vinblastine are present in the buffer, relative to vinblastine alone. In fact, in the presence of 10^{-4} M vinblastine, tubulin precipitated if the Mg^{2+} concentration in the solution exceeded 5×10^{-3} M. More recently, Frigon & Timasheff (1975a,b) have shown that tubulin isolated by the modified Weisenberg method binds Mg^{2+} and self-associates into a cyclic structure of 26 ± 4 tubulin dimers. If the two self-association reactions involve totally independent domains on the surface of the protein, it is possible that, in the presence of both ligands, tubulin can undergo both the vinblastine-induced linear, isodesmic polymerization and the Mg^{2+}-induced self-association. The structure resulting from such associations may very well be three dimensional and lead to large networks. In this regard, it is interesting to note that a number of in vitro studies have reported spiral, coiled, or even tubular structures of tubulin aggregates formed when both Mg^{2+} and vinblastine were present (Bensch et al., 1969; Marantz & Shelanski, 1970; Warfield & Bouck, 1974). Furthermore, it has been proposed that the vinblastine-induced tubulin paracrystals are actually hexagonally packed tubules which are composed of two identical helices 180° out of phase with each other (Bensch & Malawista, 1968; Fugiwara & Tilney, 1975). Fujiwara & Tilney (1975) have also suggested that the helices are composed of linearly arranged tubulin dimers. The relation, if any, between the linear, isodesmically associated tubulin polymers described in this paper and the helical tubulin polymers observed by Fujiwara & Tilney (1975) in the in vivo vinblastine-induced tubulin paracrystals is unclear at present. Since both vinblastine and Mg^{2+} are essential for the formation and stabilization of tubulin paracrystals (Wilson et al., 1978), the answer to the above question should be sought from an examination of tubulin self-association in the simultaneous presence of both vinblastine and Mg^{2+}. Such a study is presently in progress in our laboratory.

Finally, a word seems necessary concerning the possible effect of pressure on the vinblastine-induced tubulin self-association. As shown in Figure 2, the sedimentation of tubulin in PG–1 $\times 10^{-4}$ M vinblastine was carried out at different rotor speeds, ranging from 40 000 to 60 000 rpm. It can be seen that there is no dependence of the weight-average sedimentation coefficient on rotor speed, all the data following the same smooth hyperbolic curve predicted by the isodesmic, indefinite self-association mechanism; i.e., the chain growth equilibrium constant is independent of speed. This suggests that the hydrostatic pressure generated during the ultracentrifugation has no significant effect on the chemical equilibrium of the self-association reaction. In PG–1 $\times 10^{-5}$ M vinblastine, where the sedimentation boundary resolves into a bimodal one, the ratio of the areas under the slow and fast moving peaks was found to change with rotor speed. This change, however, need not reflect the effect of hydrodynamic pressure on the macromolecular equilibrium. Cann & Goad (1972) have shown that when a bimodal sedimentation boundary is generated by a concentration gradient of free ligand, the ratio of the areas under the slow and fast moving peaks generally does not reflect the chemical equilibrium of the self-association. A change in rotor speed affects the transport of both monomers and polymers which results in the generation of nonidentical gradients of free ligand across the boundary at different speeds. Since here the bimodal boundary is established by such gradients, its shape must be a function of rotor speed.

References

Behnke, O., & Forer, A. (1972) *Exp. Cell Res. 73*, 506–508.

Bensch, K. G., & Malawista, S. E. (1968) *Nature (London) 218*, 1176–1177.

Bensch, K. G., & Malawista, S. E. (1969) *J. Cell Biol. 40*, 95–107.

Bensch, K. G., Marantz, R., Wisniewski, H., & Shelanski, M. (1969) *Science 165*, 495–496.

Bhattacharyya, B., & Wolff, J. (1976) *Proc. Natl. Acad. Sci. U.S.A. 73*, 2375–2378.

Bryan, J. (1971) *Exp. Cell Res. 66*, 129–136.

Bryan, J. (1972a) *J. Mol. Biol. 66*, 157–168.

Bryan, J. (1972b) *Biochemistry 11*, 2611–2616.

Cann, J. R., & Goad, W. B. (1970a) in *Interacting Macromolecules*, Academic Press, New York and London.

Cann, J. R., & Goad, W. B. (1970b) *Science 170*, 441–445.

Cann, J. R., & Goad, W. B. (1972) *Arch. Biochem. Biophys. 153*, 603–609.

Cann, J. R., & Kegeles, G. (1974) *Biochemistry 13*, 1868–1874.

Chun, P. W., & Kim, S. J. (1969) *Biochemistry 8*, 1633–1643.

Chun, P. W., Kim, S. J., Stanley, C. A., & Ackers, G. K. (1969) *Biochemistry 8*, 1625–1632.

Cox, D. J. (1978) *Methods Enzymol. 48*, 212–242.

Cutts, J. H. (1961) *Cancer Res. 21*, 168–172.

Cutts, J. H., Beer, C. T., & Noble, R. L. (1960) *Cancer Res. 20*, 1023–1031.

Dales, S., Hsu, K. C., & Nagayama, A. (1973) *J. Cell Biol. 59*, 643–660.

Detrich, H. W., III, & Williams, R. C., Jr. (1978) *Biochemistry 17*, 3900–3907.

Frigon, R. P., & Lee, J. C. (1972) *Arch. Biochem. Biophys. 153*, 587–589.

Frigon, R. P., & Timasheff, S. N. (1975a) *Biochemistry 14*, 4559–4566.
Frigon, R. P., & Timasheff, S. N. (1975b) *Biochemistry 14*, 4567–4573.
Fujiwara, K., & Tilney, L. G. (1975) *Ann. N.Y. Acad. Sci. 253*, 27–50.
Gethner, J. S., Flynn, G. W., Berne, B. J., & Gaskin, F. (1977) *Biochemistry 16*, 5776–5781.
Gilbert, G. A. (1955) *Discuss. Faraday Soc. No. 20*, 68–71.
Gilbert, G. A. (1959) *Proc. R. Soc. London, Ser. A 250*, 377–388.
Gilbert, G. A. (1963) *Proc. R. Soc. London, Ser. A 276*, 354–366.
Gilbert, L. M., & Gilbert, G. A. (1973) *Methods Enzymol. 27*, 273–296.
Goldberg, R. J. (1953) *J. Phys. Chem. 57*, 194–202.
Himes, R. H., Kersey, R. N., Heller-Bettinger, I., & Samson, F. E. (1976) *Cancer Res. 36*, 3798–3802.
Holloway, R. R., & Cox, D. J. (1974) *Arch. Biochem. Biophys. 160*, 595–602.
Johnson, I. S., Wright, H. F., Svoboda, G. H., & Vlantis, J. (1960) *Cancer Res. 20*, 1016–1022.
Josephs, R., & Harrington, W. F. (1968) *Biochemistry 7*, 2834–2847.
Krishan, A., & Hsu, D. (1971) *J. Cell Biol. 48*, 407–410.
Lee, J. C., & Timasheff, S. N. (1974) *Biochemistry 13*, 257–265.
Lee, J. C., & Timasheff, S. N. (1975) *Biochemistry 14*, 5183–5187.
Lee, J. C., & Timasheff, S. N. (1977) *Biochemistry 16*, 1754–1764.
Lee, J. C., Frigon, R. P., & Timasheff, S. N. (1973) *J. Biol. Chem. 248*, 7253–7262.
Lee, J. C., Harrison, D., & Timasheff, S. N. (1975) *J. Biol. Chem. 250*, 9276–9282.
Malawista, S. E., & Sato, H. (1969) *J. Cell Biol. 42*, 596–599.
Marantz, R., & Shelanski, M. L. (1970) *J. Cell. Biol. 44*, 234–238.
Na, G. C., & Timasheff, S. N. (1978) *Biophys. J. 21*, 22a.
Na, G. C., & Timasheff, S. N. (1980) *Biochemistry* (following paper in this issue).
Nagayama, A., & Dales, S. (1970) *Proc. Natl. Acad. Sci. U.S.A. 66*, 464–471.
Owellen, R. J., Hartke, C. A., Dickerson, R. M., & Hains, F. O. (1976) *Cancer Res. 36*, 1499–1502.
Palmer, C. G., Livengood, D., Warren, A. K., Simpson, P. J., & Johnson, I. S. (1960) *Exp. Cell Res. 20*, 198–265.
Reisler, E., Pouyet, J., & Eisenberg, H. (1970) *Biochemistry 9*, 3095–3102.
Schachman, H. K. (1959) in *Ultracentrifugation in Biochemistry*, Academic Press, New York and London.
Townend, R., Winterbottom, R. J., & Timasheff, S. N. (1960) *J. Am. Chem. Soc. 82*, 3161–3168.
Warfield, R. K. N., & Bouck, G. B. (1974) *Science 186*, 1219–1220.
Warwick, O. H., Darte, J. M. M., & Brown, T. C. (1960) *Cancer Res. 20*, 1032–1040.
Weisenberg, R. C., & Timasheff, S. N. (1970) *Biochemistry 9*, 4110–4116.
Weisenberg, R. C., Borisy, G., & Taylor, E. (1968) *Biochemistry 7*, 4466–4479.
Wilson, L., Creswell, K. M., & Chin, D. (1975) *Biochemistry 14*, 5586–5592.
Wilson, L., Morse, A. N. C., & Bryan, J. (1978) *J. Mol. Biol. 121*, 255–268.
Wyman, J. (1964) *Adv. Protein Chem. 19*, 224–285.